Desmoplakin is required for microvascular tube formation in culture

Xuan Zhou[1], August Stuart[2], Luis E. Dettin[1], Gisela Rodriguez[1], Bonnie Hoel[1] and G. Ian Gallicano[1,*]

[1]Department of Cell Biology and [2]Interdisciplinary Tumor Biology Program, Lombardi Comprehensive Cancer Center, Georgetown University Medical Center, 3900 Reservoir Road NW, Washington, DC 20007, USA

*Author for correspondence (e-mail: gig@georgetown.edu)

Accepted 30 January 2004
Journal of Cell Science 117, 3129-3140 Published by The Company of Biologists 2004
doi:10.1242/jcs.01132

Summary

Desmoplakin (DP) is a key component of cellular adhesion junctions known as desmosomes; however, recent investigations have revealed a novel location for DP in junctions separate from desmosomes termed complexus adherens junctions. These junctions are found at contact sites between endothelial cells that line capillaries. Few studies have focused on the function of DP in de novo capillary formation (vasculogenesis) and branching (angiogenesis) during tumorigenesis, embryonic development, cardiovascular development or wound healing. Only recently have investigations begun to determine the effect the loss of DP has on capillaries during embryogenesis (i.e. in DP$^{-/-}$ mice). Evidence shows that the loss of desmoplakin in vivo results in leaky capillaries and/or capillary malformation. Consequently, the goal of this study was to determine the function of DP in complexus adherens junctions during capillary formation. To accomplish this goal, we used siRNA technology to knock down desmoplakin expression in endothelial cells before they were induced to form microvascular tubes on matrigel. DP siRNA treated cells sent out filopodia and came in close contact with each other when plated onto matrigel; however, in most cases they failed to form tubes as compared with control endothelial cells. Interestingly, after siRNA degradation, endothelial cells were then capable of forming microvascular tubes. In depth analyses into the function of DP in capillary formation were not previously possible because the tools and experimental approaches only recently have become available (i.e. siRNA). Consequently, fully understanding the role of desmoplakin in capillary formation may lead to a novel approach for inhibiting vasculo- and angiogenesis in tumor formation.

Key words: Desmoplakin, Cell adhesion, Capillary, VE-Cadherin, Endothelial

Introduction

Angiogenesis has been shown to play a pivotal role in tumor growth, and has emerged over the past decade as a promising target for anti-cancer therapies. Yet on a molecular level, much is still unknown about the process of microvascular formation during tumorigenesis, normal embryonic development or wound healing. One avenue of research that has emerged to the forefront of the angiogenesis field involves investigating the cytoskeletal components and cell adhesion junctions that endothelial cells must create to form capillaries (Dejana et al., 1995; Dejana et al., 1999; Dejana, 1996; Kowalczyk et al., 1998; Ilan et al., 2000; Gallicano et al., 2001; Davis et al., 2002; Leach et al., 2002; Calkins et al., 2003). The rationale for this approach extends from certain cell adhesion proteins that endothelial cells have used to form junctions unique to capillaries (Kowalczyk et al., 1998; Bazzoni et al., 1999; Yang et al., 1999; Gallicano et al., 2001; Venkiteswaran et al., 2002). One endothelial cell junction that has recently gained much attention is the complexus adherens junction (Schmelz et al., 1993; Schmelz et al., 1994; Valiron et al., 1996; Kowalczyk et al., 1998; Gallicano et al., 2001; Calkins et al., 2003). Its restriction to endothelial cells that comprise capillaries and lymph vessels (Schmelz et al., 1993; Schmelz et al., 1994; Dejana, 1996; Gallicano et al., 2001; Calkins et al., 2003) has made the components of this junction prime candidates for targeting and disruption of angiogenesis in tumorigenesis.

Desmoplakin (DP), a major constituent of desmosomal junctions, has been proposed to play a role in the formation of the complexus adherens junctions (Schmelz et al., 1993; Schmelz et al., 1994; Kowalczyk et al., 1998; Gallicano et al., 2001; Catellino et al., 2003). Evidence shows that DP links vascular endothelial cadherin (VE-Cad) to the vimentin intermediate filament network through one of two intermediary armadillo proteins, p0071 (plakophilin 4; Calkins et al., 2003), or plakoglobin (Valiron et al., 1996; Kowalczyk et al., 1998; Venkiteswaran et al., 2002; Cattelino et al., 2003). However, while a handful of recent investigations have determined roles for VE-Cad, p0071 and plakoglobin in capillary formation and stabilization, few investigations have focused on the role and regulation patterns of desmoplakin in de novo capillary formation (vasculogenesis) and branching (angiogenesis). Consequently, DP function in vasculo- and angiogenesis remains poorly understood.

Previously, we showed that ablation of DP in vivo produced mouse embryos with what appeared to be leaky and/or poorly formed capillaries, limiting embryonic development (Gallicano et al., 2001). Capillaries in DP$^{-/-}$ embryos were sparse and those that did form showed evidence of rupturing.

Consequently, that work led to a novel hypothesis: DP is a crucial component of capillary formation.

To test this hypothesis and further investigate the role of DP in angiogenesis, we utilized two model systems: a human microvascular endothelial cell line (HMEC-1) and a mouse yolk sac-derived cell line (C166 cells). When cultured on matrigel and treated with vascular endothelial growth factor (VEGF), both HMEC-1 cells and C166 cells combine to form microvascular tubes with similar dimensions and markers as capillaries, making them a good in vitro model for investigating aspects of vasculo- and angiogenesis (Haar and Ackerman, 1971; Ades et al., 1992; Pruckler et al., 1993; Bosse et al., 1993; Xu et al., 1994; Lu et al., 1996; Wang et al., 1996).

To determine the role of DP in capillary formation/stabilization, we used a relatively new technology, RNA interference using small interfering RNAs (siRNA), to knock down the levels of DP expressed in HMEC-1 and C166 cells. Here, we show that DP siRNA transiently inhibits the ability of HMEC-1 cells and C166 cells to form proper and stable microvascular tubes.

Materials and Methods

Cell lines, media and tissue procurement

HMEC-1 were used with permission from Francisco Candal (Center for Disease Control and Prevention, Atlanta, GA). These cells have been immortalized by the SV40 large T antigen driven by the Rous Sarcoma Virus long terminal repeat (Ades et al., 1992). The cells were grown in tissue culture dishes in EGM-2 medium (EBM-2 supplemented with MV singlequot; Clonetics cat# CC-3156 and CC-4147). The Singlequot contains 5% FBS, hydrocortisone, human fibroblast growth factor (hFGF-8), VEGF, insulin-like growth factor (IGF), ascorbic acid and hEGF. C166 cells were used with permission from Robert Auerbach (University of Wisconsin, Madison, WI). These cells were isolated from yolk sacs of mice containing a mutant allele of the human fps/fes proto-oncogene, which encodes a hyperactive Fps/Fes cytoplasmic protein tyrosine kinase. The cells are normally grown in tissue culture dishes in Dulbecco's Modified Eagle's Medium (DMEM) + 10% FBS (Invitrogen, Carlsbad, CA). To form microvascular tubes, each cell line was grown to 70-90% in a monolayer, followed by trypsinization and plating onto a thin layer of matrigel, a kind gift from Hynda Kleinman (National Institutes of Health). It has been well documented that microvascular endothelial cells plated onto matrigel form microvascular tubes with well-formed lumens (Maru et al., 1998; Connolly et al., 2002; Davis et al., 2002). Both HMEC-1 cells and C166 cells also form tubes with lumens (see Results).

To analyze DP distribution in capillaries in vivo, yolk sacs were acquired from E9.5-day embryos after dissection of embryos and extraembryonic tissues from deciduas. Before embryo dissection, pregnant female mice were killed by asphyxiation using CO_2. Yolk sac tissue was frozen in OCT compound, sectioned at 7-8 μm onto glass slides using a cryomicrotome and fixed in cold methanol for 10 minutes. After fixation, specimens were processed for immunohistochemistry using standard procedures (see below). Rat skin was analyzed for DP expression after CO_2 asphyxiation of 12-day-old rat pups. Small pieces of skin and tail were placed into OCT compound and rapidly frozen. Specimens were sectioned onto a glass slide using a cryomicrotome, fixed in cold methanol and processed for immunohistochemistry.

siRNA analysis

siRNA was produced using two different methods. First, the Dicer siRNA Generation Kit was used to generate siRNA after amplifying a 747 bp region near the transcription start site of DP cDNA. Primer sequences for DP were obtained from mouse and human DP sequence accession numbers. Primer sequences were (5′ctagtgtcaaaccggcacgatgtc3′) for the 5′ primer and (5′ttggtgttcttgtcgctccagtcg3′) for the 3′ primer. Each primer set could amplify the proper size band of 747 bp from 1:1000 dilution of cDNA. This amplicon was converted to double-stranded RNA (dsRNA) and then diced into 21 bp fragments using a recombinant human dicer enzyme following the manufacturer's protocol (Gene Therapy Systems, San Diego, CA). siRNA was then transfected into HMEC-1 or C166 cells where they produced sequence-specific inhibition at the mRNA, leading to downregulation of its specified protein as measured by western blot. A GFP expression vector and corresponding GFP-specific dsRNA was used as a control. To generate siRNA using a different method, we sent to Dharmacon the accession numbers for human (BC033467) and mouse (NM_004415) DP, with which they proceeded to generate a pool of 19 bp oligomers that recognized both mouse and human mRNA. The oligomer sequences that comprise pool number M-003944-00 are: tcaaagtcctggagcaaga, gcatccagcttcagacaaa, acaccaacatcgctcagaa and gtgcagaacttggtaaaca. To determine the best concentration of siRNA for DP inhibition we generated a standard curve whereby HMEC-1 or C166 cells were incubated in 0 nM, 10 nM, 100 nM and 200 nM, followed by assaying for tube formation and protein expression. Western blots of cells were used to determine the relative inhibition of DP at each siRNA concentration in HMEC-1 and C166 cells (data not shown).

RT-PCR

C166 or HMEC-1 cell monolayers were washed in DEPC phosphate-buffered saline (PBS), scraped from the cell culture dish and immediately placed into Trizol reagent (Life Technologies, Gaithersburg, MD) to isolate RNA. RT-PCR was carried out using the Onestep RT-PCR kit (Life Technologies). Two microliters of RNA was pipetted into a 20 μl RT-PCR reaction mixture containing 1× RT-PCR buffer, 40 ng of each primer, optimal concentration of $MgCl_2$, 0.2 mM dNTPs, and 2 U of reverse transcriptase and Taq polymerase. Primer sequences for DP were the same as described for generating siRNA. Each primer set amplified the proper size band of 747 b.p. from 1:1000 dilution of cDNA product from an RT reaction of 1 μg total RNA isolated from each cell line. The DNA template was denatured at 94°C, followed by amplification using the following parameters: 94°C for 20 seconds, 59°C for 45 seconds, and 72°C for 1 minute, for 40 cycles. Control RT-PCR reactions were run for each batch of mRNA. First, no RT was used in concurrent reactions to determine if contaminating DNA was present. Second, DP primers were generated from two different exons (5′ primer-exon 1/2 and for the 3′ primer-exon 7). The rationale for this approach is that amplification of contaminating genomic DNA would result in a PCR product with a molecular weight much higher than a PCR product amplified from cDNA. Third, tubulin primers were used as a positive control for all PCR reactions. Ten-microliter aliquots of each PCR product were electrophoresed on a 2% agarose gel and visualized using ethidium bromide.

Immunohistochemistry and immunofluorescence

Monolayers of cells were fixed in either 100% methanol at –20°C for 10 minutes or in Tris-buffered saline (TBS) containing 4.0% paraformaldehyde for 20 minutes, followed by permeabilization in TBS supplemented with 1.0% Tween-20 for 20 minutes at room temperature. Microvascular tubes were individually picked from their matrigel beds using a microneedle. Each microvascular tube was pipetted into a 35 mm dish containing TBST + 10% protein diluent from the mouse on mouse kit (M.O.M., Novacastra, CA), which served as blocking agent. Nonspecific antigen sites were blocked for 1 hour at room temperature, after which they were transferred to

blocking agent containing the appropriate dilution of antibody (see below). Incubation times for all antibodies were overnight at 4°C. The next day, tubes were transferred to three washes of blocking agent for 30 minutes each wash, followed by incubation for 1 hour at room temperature in blocking agent containing the appropriate dilution of secondary antibody. Tubes were then washed in TBST three times for 30 minutes each, mounted onto glass slides with antifade and covered with a glass coverslip. Specimens were viewed using standard phase optics and an Olympus FV500 confocal microscope.

Antibodies used were anti-DP 2.15 (AARP) at 1:25, anti-VE-Cad (Santa Cruz Biotechnology, Santa Cruz, CA) at 1:50 and anti-vimentin (Santa Cruz) at 1:100. All secondary antibodies (fluorescently labeled or biotinylated) were used at 1:500.

Western blot analysis

Microvascular tubes or cell monolayers were immediately placed into sample buffer (62.5 mM Tris-HCl, pH 6.8, 2% SDS w/v, 1 mM β-mercaptoethanol, 10% glycerol). Samples were boiled for 5 minutes and loaded onto 10% polyacrilamide gels with molecular weight markers and separated by SDS-PAGE. Proteins were transferred to PVDF membrane and blocked with blotto (5% dry milk in PBS, pH 7.4, with 0.1% Tween 20) at room temperature. The blots were challenged with primary antibody at dilutions of 1/500-1/1000 in blotto overnight at 4C, followed by washing three times with PBT (1×PBS + 0.1% Tween 20) at room temperature and challenged with appropriate secondary antibody conjugated to horseradish peroxidase (Pierce, Rockford, IL). As a positive control, tissue samples known to contain desmoplakin were always loaded in a subsequent lane to verify the efficacy of the anti-DP used for each experiment.

Electron microscopy

Ultrastructural analyses were carried out similarly to that described in Gallicano et al. (Gallicano et al., 1998). Briefly, cells/tubes on matrigel were scraped off the bottom of the culture dish and pipetted into Eppendorf tubes, washed three times with PBS and fixed at room temperature for >1 hour. Fixative consisted of 0.2 M sodium cacodylate buffer, pH 7.4, containing 2.5% gluteraldehyde and 2% formaldehyde. Cells/tubes were washed three times in the same buffer without fixative, followed by postfixation in buffer containing 1% aqueous osmium tetroxide for 1 hour at room temperature. Cells/tubes were then dehydrated in ascending grades of ethanol and propylene oxide. Samples were embedded in Epon, polymerized at 70°C for 48 hours, trimmed, sectioned at 90 nm, post-stained in 50% saturated uranyl acetate and 0.2% lead citrate, and examined with an Hitachi H7600 transmission electron microscope.

Data analysis

Images of microvascular tubes were obtained using a Nikon Coolpix 990 digital camera. Tubes were counted in a 1 cm^2 area from at least three wells of a 24-well dish per experiment. Each DPsiRNA experiment was done on both C166 cells and HMEC-1 cells. Tubes also were measured in 1 cm^2 areas in 60 mm dishes. Tube number and tube length were calculated from each cell line from at least three experiments, which generated a mean±standard error of the mean (s.e.m.), which were then graphed.

Results

Desmoplakin is localized to endothelial cell-cell junctions after formation of microvascular tubes

Desmoplakin has been shown to localize at cell-cell contacts within complexus adherens junctions in endothelial cells that comprise capillaries (Valiron et al., 1996; Kowalczyk et al., 1998; Gallicano et al., 2001; Calkins et al., 2003). It has also been shown more recently that DP, when transfected into endothelial cells, colocalizes with VE-Cad and the armadillo family member p0071 at the plasma membrane, presumably at nascent complexus adherens junctions (Kowalczyk et al., 1997; Kowalczyk et al., 1998; Calkins et al., 2003). However, to date, a view of DP expression and localization in endothelial cells during and after the formation of microvascular networks has not been detailed. Consequently, determining the gene and protein expression profile of DP was crucial for determining the function of DP in microvascular tube formation.

The two cell lines, HMEC-1 (Ades et al., 1992; Pruckler et al., 1993; Bosse et al., 1993; Xu et al., 1994) and C166 (Wang et al., 1996), were specifically chosen because: (1) both form microvascular tubes beginning ~5 hours after plating onto a thin layer of matrigel; (2) each cell line has been well characterized as behaving like and containing capillary-specific markers; (3) both have been immortalized, allowing for long-term analysis (>10 days) of microvascular tubes; (4) analysis of tube formation in endothelial cell lines from two different species and from two different organ structures (human dermal tissue for HMEC-1 and mouse yolk sac for C166 cells) would support or refute an argument of universality for DP function in capillaries.

We first determined the subcellular localization pattern of DP in vivo and in culture. It has been shown that DP is expressed in dermal capillary cells in culture (Valiron et al., 1996; Kowalczyk et al., 1998; Venkiteswaran et al., 2002); however, few reports have shown distinct localization of DP in the dermal capillaries or the yolk sac. As seen in Fig. 1, in dermal capillaries in vivo, DP was consistently observed directly juxtaposed with VE-Cad. Nearby hair follicles served as internal controls for DP antibody binding where it is found in desmosomes adhering cells within hair follicles (Kurzen et al., 1998; Norgett et al., 2000; Hatsell and Cowin, 2001; Vasioukhin et al., 2001). DP also was present in the microvasculature within the 9-day-old mouse yolk sac. It localized primarily within the newly formed microvasculature and was observed closely associated with the vimentin intermediate filament network (Fig. 1C-F), as well as other capillary markers including VE-Cad and platelet-endothelial cell adhesion molecule (PECAM) (data not shown). Interestingly, immunohistochemical and immunofluorescent analyses of cell lines derived from these two tissue types showed little DP staining at cell-cell junctions when each were grown in monolayers (Fig. 2). However, after both cell lines were induced to form tubes by plating on matrigel, DP was observed primarily at cell-cell contacts colocalized with VE-Cad (Fig. 2). Detection of DP at cell-cell contacts normally occurred ~12-24 hours after tube formation. HMEC-1 and C-166 cells routinely formed microvascular tubes with lumens (Fig. 2C inset); however, lumens were usually observed embedded within the matrigel, which made it difficult to see them using DIC (not shown) or phase contrast light microscopy (Fig. 2C).

Using RT-PCR, we determined the expression pattern of the DP gene in both cell lines (Fig. 3). Interestingly, although little DP was detected at cell-cell contacts when grown in monolayers (Fig. 2), DP transcripts were routinely detected in monolayers of HMEC-1 lines. This observation persisted in both subconfluent (~50-90%) and confluent cultures. In yolk

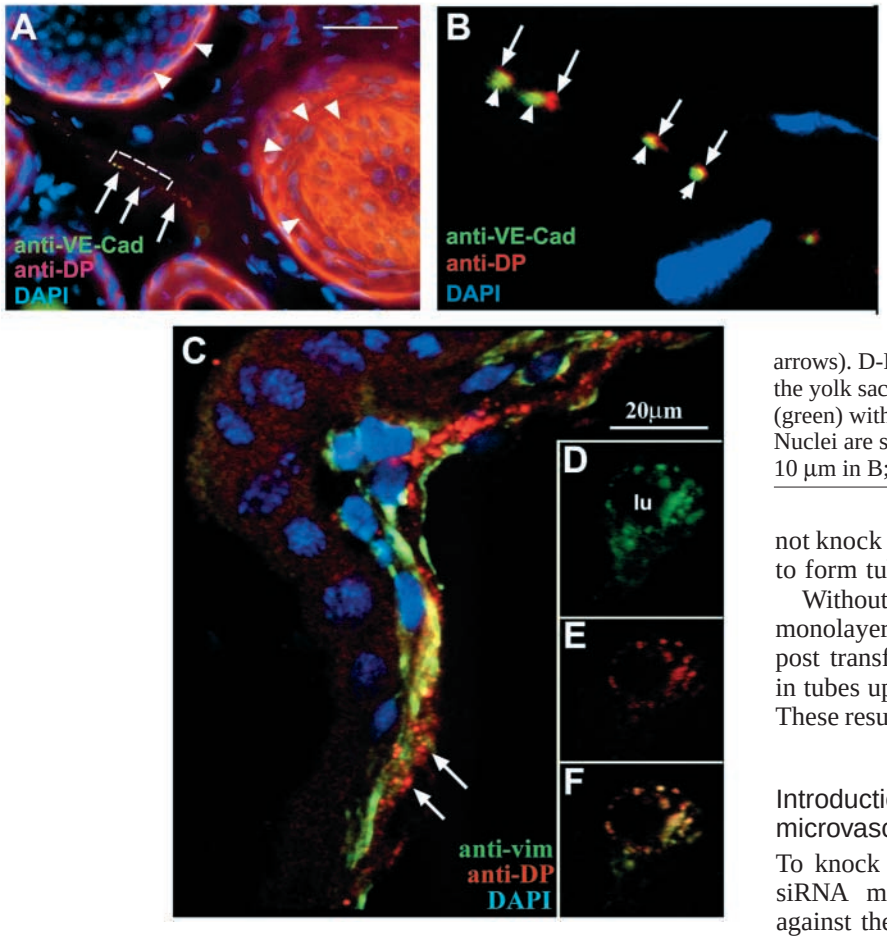

Fig. 1. Localization of DP within capillaries was analyzed by immunofluorescence. (A) Dermal capillary (arrows) in rat skin is recognized by antibodies to VE-Cad (green) and DP (red). Arrowheads point to DP staining within desmosomes that are involved in adhering cells within hair follicles including inner and outer root sheath cells. (B) High magnification of area outlined in A shows that DP (red; arrows) is localized directly adjacent to VE-Cad (green; arrowheads). (C) Confocal view of an E9 day mouse yolk sac shows vimentin (green) associated with DP (red; arrows). D-F are cross-sectional, high-magnification views of the yolk sac that show the close association in F of vimentin (green) with DP (red) surrounding the capillary lumen (lu). Nuclei are stained with DAPI in each figure. Bar in A=100 μm; 10 μm in B; 50 μm in C.

sac-derived C166 cells, however, DP transcripts were rarely detected in cells grown in monolayers (Fig. 3). This expression pattern changed, however, as DP transcripts were routinely detected as soon as 1.5 hours after plating cells onto matrigel, before they formed tubes. On closer inspection, we found that DP gene expression in C166 cells was reliant on growth in the proper medium. We expand on these data below.

Introduction of CMV-GFP and GFP siRNA into endothelial cells results in GFP suppression without detrimental affects to microvascular tube formation

To determine the function of DP in microvascular tube formation, we set out to knock down DP translation using siRNA technology. However, because few studies existed describing siRNA introduction into microvascular endothelial cells and none existed for our two cell lines, it was imperative to determine the efficacy of siRNA inhibition of mRNA transcripts. To do so, we cotransfected in HMEC-1 cells GFP driven by a CMV promoter and siRNA specific for GFP. Fig. 4 shows that in HMEC-1 monolayers GFP siRNA significantly inhibited GFP expression, an inhibition that lasted at least 72 hours (data not shown). GFP inhibition persisted in these cells even after they had formed microvascular tubes (Fig. 4A-D). One important observation from this experiment was the specificity of GFP siRNA. These cells were still capable of making tubes even in the presence of 250 ng siRNA, suggesting that GFP siRNA did not knock down other messages necessary for these cells to form tubes.

Without GFP siRNA, at least 70% of HMEC-1 cells in monolayers were positive for GFP as soon as 24 hours post transfection (Fig. 4E-F). GFP expression persisted in tubes up to 84 hours post tube formation (Fig. 4G-H). These results were similar in C166 cells (data not shown).

Introduction of DP siRNA results in malformed microvascular tubes

To knock down DP expression, we used two different siRNA methodologies. First, we synthesized siRNA against the first 747 bp of the human DP mRNA using the Dicer siRNA Generation Kit and protocol from Gene Therapy Systems (Kawasaki et al., 2003; Myers et al., 2003). Second, a pool of siRNA specific to both mouse and human DP was synthesized and processed by Dharmacon. Although the two methods for producing siRNA were different, the results observed using both methods in both endothelial cell types were equivalent.

Fig. 5 shows the effects of DP siRNA in HMEC-1 cells. In monolayers that were 75-80% confluent, no effect was observed at any time post transfection with DP siRNA. HMEC-1 cells were incubated in DP siRNA for 24-48 hours to allow for optimum downregulation of DP translation, after which the cells were trypsinized and plated either 1:1 or 1:2 into wells (48-well plate) at a density of ~1×10^3 cells per well. In untreated, wild-type cells, microvascular tubes usually began forming 4-5 hours after plating. By contrast, by 5 hours, few microvascular tubes were observed forming from cells that had been treated with DP siRNA (Fig. 5E1-4). Video analysis revealed cells migrating towards each other, followed by their close contact; however, they rarely adhered to one another or elongated into tube-like structures (see below).

By 12 hours a significant difference was visible between treated and untreated cells (Fig. 5B,F) (quantified in Fig. 10): microvascular tubes were prevalent by 12 hours in control cells, whereas cells treated with DP siRNA resulted in significant inhibition in microvascular tube formation. Control cells were treated identically to those treated with siRNA except that siRNA was not added to transfection reagents in control cells. However, as shown in Fig. 4, a GFP siRNA

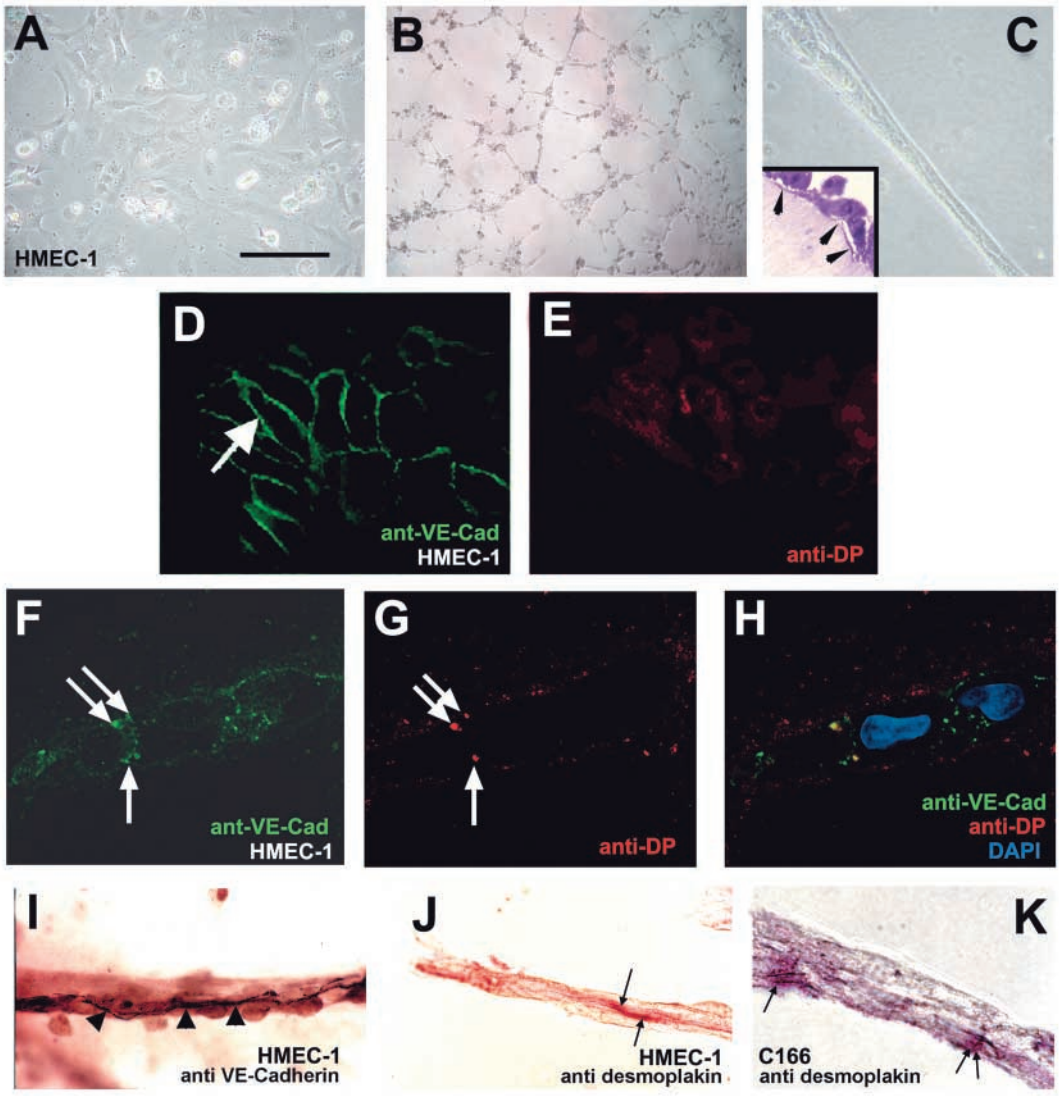

Fig. 2. DP protein localization was characterized in HMEC-1 and C166 cells. (A-C) HMEC-1 cells grow as monolayers in tissue culture dishes; however, ~5 hours after plating onto matrigel they form microvascular tubes (B,C). Inset in C is a toludine blue, semithin section of a microvascular tube grown on matrigel in culture. The lumen (arrows) in these tubes is usually found embedded in the matrigel. In monolayers VE-Cad is localized to cell membranes (D; arrow), while DP (E) appears to be cytoplasmic. (F,G) Once plated onto matrigel, VE-Cad (F) and DP (G) colocalize with one another (H). I and J show morphologically and immunohistochemically the localization pattern of VE-Cad (I; arrowheads) and DP (J; arrows) in microvascular tubes. (K) DP also is localized to cell-cell contacts in C166 microvascular tubes. Note: the microvascular tube shown in F-H is morphologically similar to those found in I-K. Bars, 100 μm (A,B); 50 μm (C and inset); 25 μm (D,E), 20 μm (F-H); 40 μm (I-K).

(representing a foreign control siRNA) did not inhibit any components necessary for tube formation as tubes were found to consistently form after treatment with this control siRNA.

To further confirm that DP siRNA knocked down DP expression leading to tube malformation, DP siRNA-treated cells plated onto matrigel (Fig. 5) were subjected to western blot analysis (Fig. 6). DP siRNA-treated cells showed that DP protein expression was downregulated to undetectable levels by 24 hours after plating onto matrigel (48 hours after the addition of DP siRNA to monolayers). This knockdown of DP persisted to 72 hours after plating (96 hours after the addition of DP siRNA to monolayers). It is possible that low levels (below detection) of DP may have been present in treated cells; however, these levels were not sufficient to allow cells to form tubes. Other components involved in complexus adherens junction formation were not affected by DP siRNA treatment (Fig. 6C-D).

The inhibition of tube formation lasted throughout the duration of the experiments until approximately 106-144 hours after plating treated cells onto matrigel, at which time these same DP siRNA-treated HMEC-1 cells proceeded to form microvascular tubes (Fig. 7A,B). This re-establishment of tube formation was presumably due to siRNA degradation as DP protein was detectable at approximately the same time points as DP siRNA treated cells were once again capable of forming microvascular tubes (Fig. 6). Note that the tube in Fig. 7B (arrows) was composed of the same set of cells as those in Fig. 5H, indicating that treating cells with DP siRNA did not result

in their lethality. Again, these data were duplicated in C166 cells (data not shown).

On closer inspection of DP siRNA-treated and untreated cells, high magnification of treated cells revealed that they were capable of locating adjacent cells by sending out filopodia (Fig. 8), an observation made in untreated cells and previous investigations (Bazzoni et al., 1999; Yang et al., 1999; Davis et al., 2000; Davis et al., 2002; Venkiteswaran et al., 2002; Kouklis et al., 2003). We observed that once contact was made, the cells migrated and came in close contact with each other, after which they adhered and formed small hollow tubes (Yang et al., 1999; Davis et al., 2000; Davis et al., 2002). In DP siRNA-treated HMEC-1 or C166 endothelial cells, while tube formation was disrupted, the process of migration was only slightly altered – that is, in some cases, many DP siRNA-treated cells remained somewhat rounded. However, time-lapse movies revealed that those rounded cells were still capable of adhering to the matrigel substrate and moving towards other cells (Fig. 8 and Fig. 5E1-5; Fig. 5H).

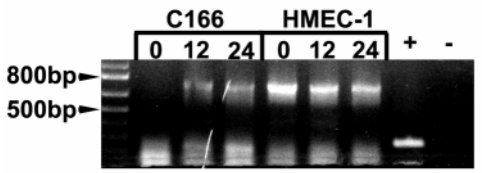

Fig. 3. RT-PCR of C166 and HMEC-1 cells grown on matrigel in growth factor containing EGM-2 medium shows DP gene expression at 12 and 24 hours in C166 cells. No DP was detected in C166 cells grown in monolayers in DMEM medium (without growth factors). Tubulin primers were used on the same time 0, C166 mRNA used in lane 1 to show presence of mRNA. +, with reverse transcriptase; –, no reverse transcriptase.

Analysis of cell-cell contacts using electron microscopy revealed distinct differences in adhesion in cells treated with DP siRNA when compared with control cells (Fig. 9). Cells treated with DP siRNA recognized each other via microvilli, a similar observation made in untreated, wild-type cells. Cells also were capable of coming in close contact with each other and even adhering to one another; however, elongation of endothelial cells did not occur in DP siRNA-treated cells as it did in control, nontreated cells or cells treated with GFP siRNA (Fig. 9). Interestingly, DP siRNA-treated cells that were in close contact with each other attempted to form lumens, suggesting that the loss of DP affected cell adhesion and not other aspects of tube formation. In essence, without DP and a complete complexus adherens junction, a distinct membrane anchorage site necessary for endothelial cell adhesion is lost, resulting in compromised microvascular tube formation.

Quantification of tube formation showed that the same number of treated cells formed far fewer microvascular tubes than control cells (Fig. 10A). The tubes that did form in treated cells were also significantly shorter than those of controls (Fig. 10B). However, by 144 hours post DP siRNA treatment, cells showed a significant level of rescue as microvascular tube numbers and length approached those of untreated control cells (Fig. 10 and Fig. 7). Evidence that DP siRNA may be degraded over time was seen in western blots as DP protein re-expression coincided with the eventual formation of tubes from cells that had been treated with DP siRNA 100 hours earlier (Fig. 6).

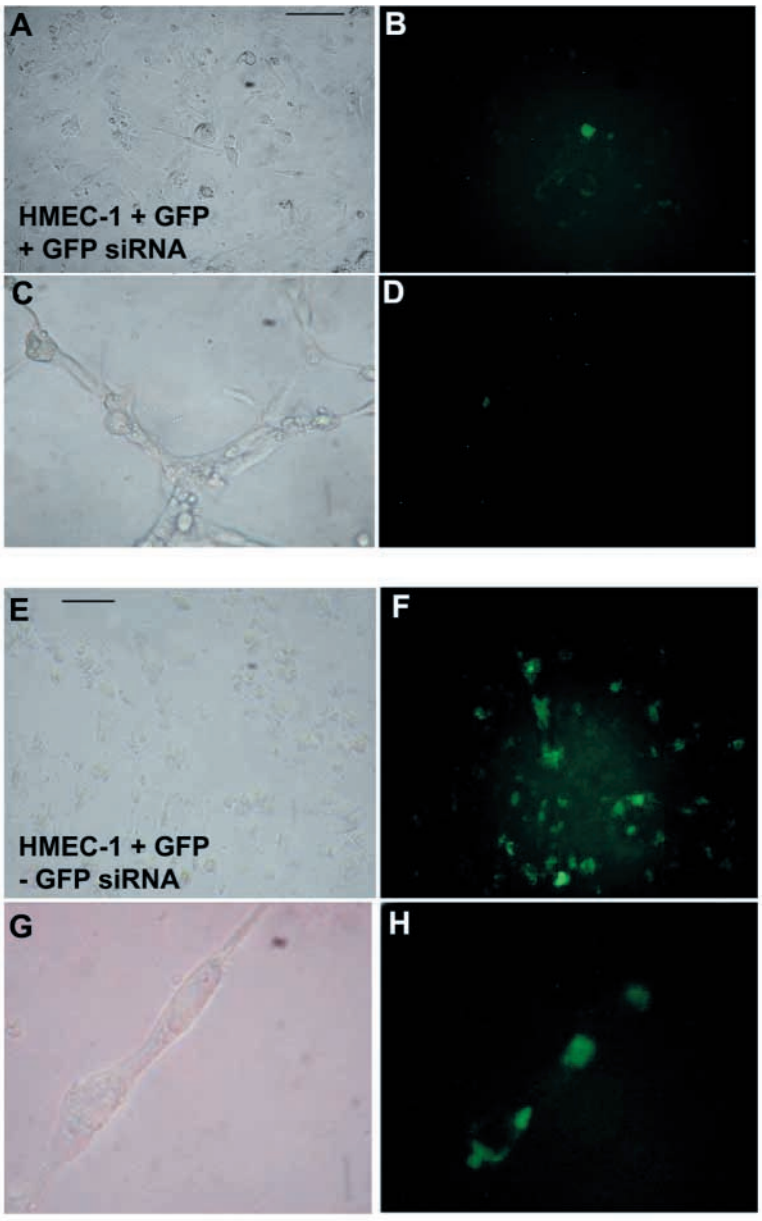

Fig. 4. To determine if siRNA functioned in HMEC-1 cells, a CMV-GFP gene and its corresponding siRNA were simultaneously transfected into a monolayer of HMEC-1cells, followed by incubation for 24 hours. A subset of these HDME-1 cells (A,B) were then placed onto matrigel and analyzed for tube formation 12-24 hours later (C,D). GFP siRNA successfully knocked down translation of GFP. Note: GFP siRNA did not affect tube formation. (E-H) As a control, GFP was expressed in HMEC-1 cells without the addition of GFP siRNA. In contrast to cells transfected with CMV-GFP and siRNA, cells without GFP siRNA were found expressing GFP both in monolayers (F) and in their corresponding tubes (H). Bar in A, for A-D, 20 μm; bar in E, for E-H, 20 μm.

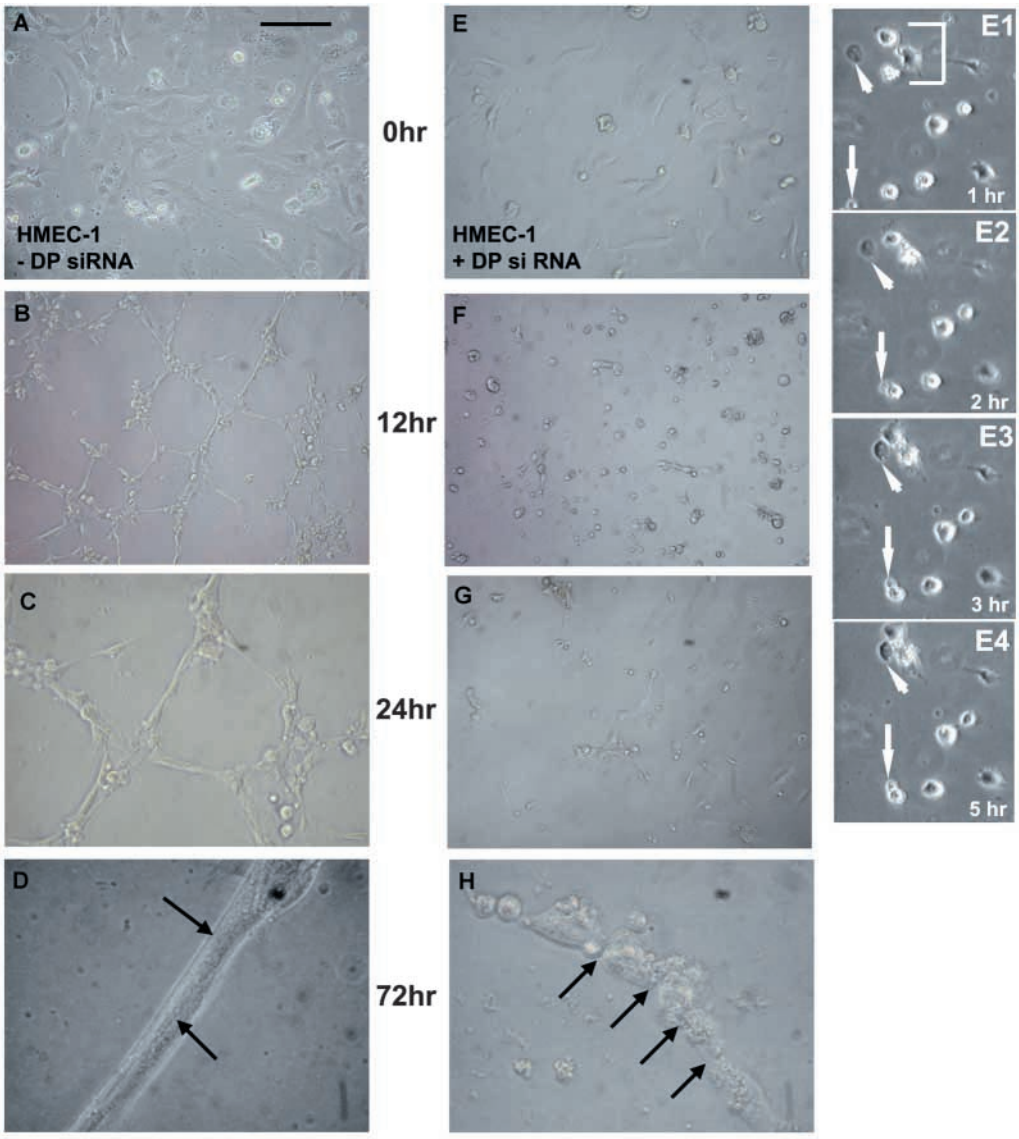

Fig. 5. Microvascular tube formation was compared in the absence and presence of DP siRNA. (A,E) HDME-1 cells in a monolayer do not form tubes. The absence (A) or presence (E) of DP siRNA did not affect the monolayer. (B-D) Cells placed onto a thin layer of matrigel form tubes after 5-8 hours, which persist up to 10 days in culture. Addition of 250 ng of DP siRNA significantly compromised tube formation (E1-4; F-H). E1-4 are four frames taken from a five hour video showing migration patterns of DP siRNA treated cells after plating onto matrigel. Four to five cells within the white bracket in E-1 are joined by a migrating cell (arrowhead E1-4) but do form a tube. The arrow in E1-4 points to another cell migrating towards a stationary cell. Adhesion between cells appears to be compromised up to 72 hours post siRNA treatment (H). Bars, 50 μm (A,B,E,F); 30 μm (C,G); 15 μm (D,H).

Desmoplakin is not expressed in endothelial cells derived from the mouse yolk sac unless they are induced to further differentiate

We found that DP expression was below levels of detection as measured by RT-PCR in monolayers of C166 cells grown in their normal DMEM + 5% FBS medium (Fig. 3). On plating these cells onto matrigel in EGM-2 medium, C166 cells consistently expressed DP by 12 hours once tubes had formed (Fig. 3). To determine if this phenomenon was due to the environment provided by incubation in EGM-2 medium, we switched monolayers of C166 cells from DMEM to EGM-2 medium for specified times, followed by RT and 40 cycles of PCR with primers specific for DP (Fig. 11). DP was not detected in monolayers of C166 cells until 1 hour 30 minutes of incubation in EGM-2 medium (Fig. 11). We concluded that endothelial cells generated from the yolk sac must be incubated in the correct media to express DP. More importantly, the correct media and three-dimensional substrate is necessary for yolk sac cells to form microvascular tubes in culture.

Discussion

Numerous laboratories (the Dejana and Kowalczyk laboratories in particular) have characterized many aspects and functions for cell adhesion molecules in endothelial cells (Dejana, 1996; Vittet et al., 1997; Maru et al., 1998; Bazzoni

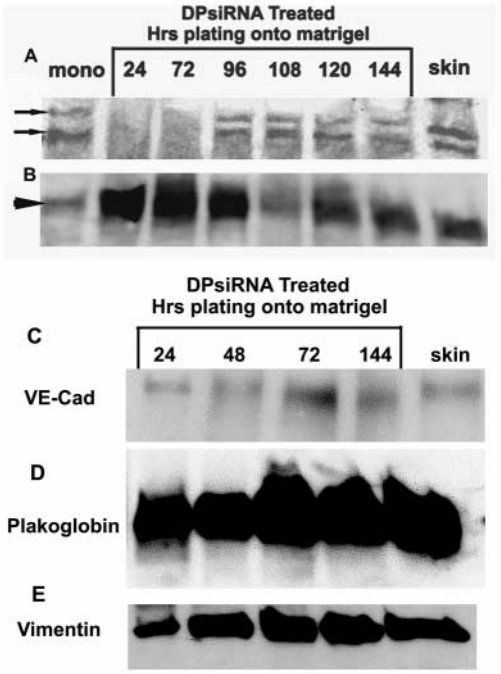

Fig. 6. Western blot shows the affect of DP siRNA. (A) DP (~250/230 kDa, arrows) is absent in siRNA-treated microvascular tubes. (B) Antibodies to tubulin were used as a loading control. Tubulin runs at ~55 kDa (arrowhead). Lane 2: monolayer no DPsiRNA. Lane 3: microvascular tubes 24 hours after plating onto matrigel (48 hours after DP siRNA treatment). Lane 4: microvascular tubes 72 hours after plating onto matrigel. Lane 5: microvascular tubes 96 hours after plating onto matrigel. Lane 6: 108 hours after plating. Lane 7: 120 hours after plating. Lane 8: 144 hours after plating. Lane 9: whole mouse skin. (C-E) Western blot showing VE-cadherin staining (C), plakoglobin (D), and vimentin (E) after incubation in DPsiRNA for specified times. C-E are from the same western blot.

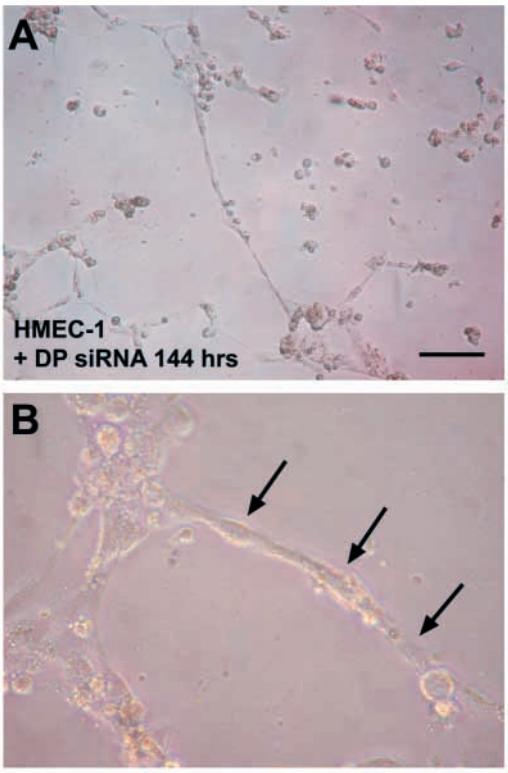

Fig. 7. HMEC-1 cells treated with DP siRNA eventually form tubes. (A) By 144 hours after cells were transfected with DP siRNA they proceeded to form microvascular tubes. (B) High-magnification view of a microvascular tube from the same set of cells in Fig. 5H that had been treated with DP siRNA shows cells adhered well to one another. Bar, 100 μm (A); 50 μm (B).

et al., 1999; Carmeliet and Jain, 1999; Ilan et al., 2000; Leach et al., 2002; Calkins et al., 2003). However, one protein that has not been thoroughly investigated and assigned a particular function (but has been repeatedly shown to reside in endothelial cells that can form microvascular tubes) is DP (Valiron et al., 1996; Kowalczyk et al., 1998; Ilan et al., 2000; Calkins et al., 2003) (this study).

In the present study, we utilized a novel technique (siRNA) to begin understanding DP function(s) in the complexus adherens junction residing at endothelial cell-cell junctions. We found that while both types of cells readily made microvascular tubes when plated onto matrigel, DP siRNA-treated cells were incapable of properly adhering to one another and forming these same types of tubes. Only after about 100 hours of siRNA treatment, once the siRNA was degraded, were treated cells capable of forming tubes. These results were not species specific as DP siRNA behaved similarly both in mouse yolk sac cells (C166) and human microvascular endothelial cells (HMEC-1).

siRNA has been well documented as a powerful tool for significantly knocking down its target messenger RNA, resulting in downregulation of its specified protein (Caplen et al., 2001; Elbashir et al., 2001; Elbashir et al., 2002). Consequently, it seemed plausible to use this technique to determine a function for DP in the formation of microvascular tubes.

Why does knocking down DP compromise vascular tube formation? The most widely accepted model for DP localization in endothelial cells is within a cell-cell attachment site termed the complexus adherens junction (Schmelz et al., 1993; Schmelz et al., 1994; Kowalczyk et al., 1998). Unlike epithelial cells (e.g. keratinocytes) where DP resides in desmosomes linking the keratin filament network to two cadherins, desmocollin and desmoglein by way of the armadillo protein, plakoglobin, DP in endothelial cells links the vimentin intermediate filament network to vascular endothelial cadherin (VE-cad) by way of p0071 (Calkins et al., 2003) or plakoglobin (Valiron et al., 1996; Kowalczyk et al., 1998; Venkiteswaran et al., 2002; Cattelino et al., 2003). From this model, we hypothesized that without DP, the vimentin IF linkage would be compromised and, like epithelial cells when DP is missing (Gallicano et al., 1998; Vasioukhin et al., 2000; Vasioukhin et al., 2001), endothelial cell adhesion would be significantly compromised, especially when they make tubes. Support for this hypothesis emerged as knocking down DP expression in endothelial cells using siRNA resulted in compromised adhesion when these cells were induced to form tubes.

However, it must be noted that the model proposed by

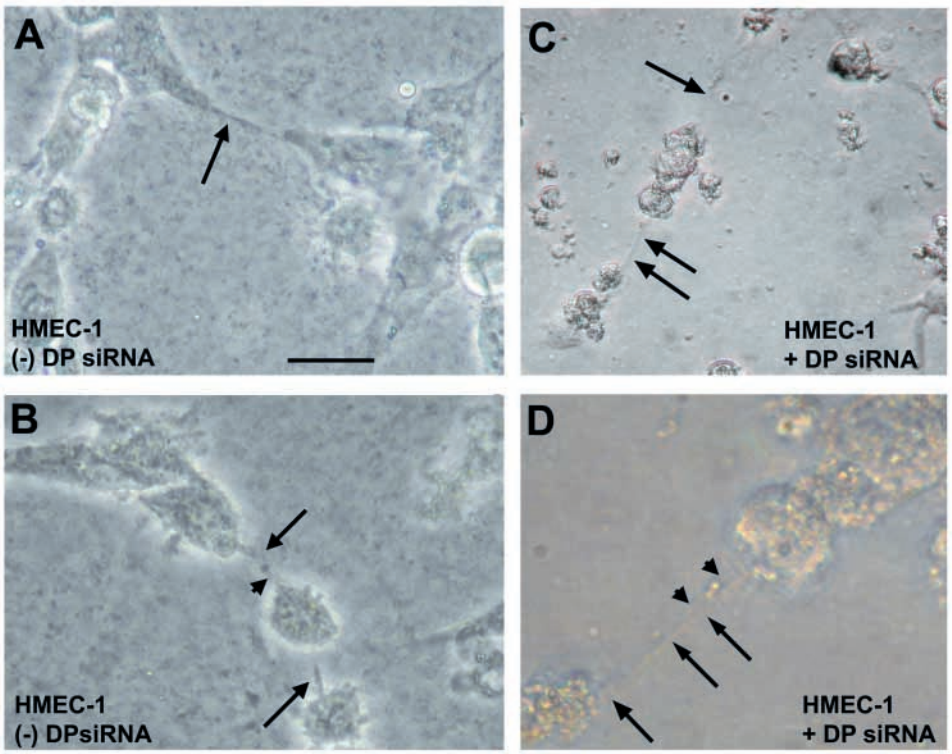

Fig. 8. Endothelial cells treated with DP siRNA are able to send out cellular projections. (A) Wild-type HMEC-1 cells send out filopodia (arrow) within 2-3 hours of plating onto matrigel. (B) Arrowhead and arrow point to filopodia from adjacent cells coming in close contact with each other. The arrowhead points to a filopodia extending from the middle cell, while the top arrow points to a filopodia extending from the top cell towards the middle cell filopodia. (C) Low-magnification view of cells treated with DP siRNA. Arrows point to long filopodia. (D) Higher magnification of cells in C show at least two filopodia. Arrows point to a filopodia extending from the lower left cell, while arrowheads point to a filopodia extending from the upper right cell. Bar, 10 μm (A, B, D); 25 μm (C).

Kowalczyk's team (Kowalczyk et al., 1998) also showed VE-cad linked to the actin filament network through an adherens junction-like set of proteins including β-catenin and α-catenin. This sparked a question as to why removing DP caused such a dramatic inhibition of tube formation if VE-Cad was still capable of adhering to the cytoskeleton through the actin filament network. One explanation could simply be that actin filaments may not be as rigid and durable as the vimentin intermediate filament network and the stresses placed on endothelial cells as they make tubes must utilize stronger cytoskeletal components (i.e. vimentin) to successfully make a tube. Alternatively, a recent investigation describing a significant relationship between PECAM and plakoglobin/β-catenin showed that PECAM also strongly associates with DP, apparently linking PECAM to the vimentin filament network (Ilan et al., 2000). This observation, along with the data presented here, strongly suggests that DP may be more promiscuous than first thought when pertaining to junction specificity. It also may be resonable to suggest that DP may indirectly enable PECAM to properly perform its function(s), one of which is recruitment of adaptor and signaling proteins. These include SHP-1, SHP-2, phospholipase Cγ, phosphoinositide 3-kinase, and beta-catenin (Hua et al., 1998; Pumphrey et al., 1999; Pellegatta et al., 1998; Matsumura, 1997; Ilan et al., 2000). Consequently, when DP is knocked out or knocked down, PECAM function may also be altered, further leading to malformation of microvascular tubes.

One very interesting observation we consistently made in this investigation was the ability of siRNA-treated cells to send out filopodia to 'search' for neighboring cells after plating onto matrigel. This observation was routine for nontreated cells plated onto matrigel. There have been a few studies showing images of endothelial cells detecting environmental surroundings by filopodia extensions (Bazzoni et al., 1999; Davis et al., 2000; Yang et al., 1999; Venkiteswaran et al., 2002; Kouklis et al., 2003). Interestingly, though, very few investigations have described in detail the process of how endothelial cells extend filopodia after plating onto matrigel. It is thought that the Cdc42 pathway may be the primary mechanism for filopodia extension in endothelial cells; however, other components such as PAK-1/stathmin also may be involved (Daub et al., 2001).

Filopodia extension has been investigated in much more detail in other cell types (e.g. epithelial cells) and may be analogous to that seen in endothelial cells. A recent investigation by Vasioukhin et al. (Vasioukhin et al., 2000) elegantly detailed the initial process of cell adhesion when two keratinocytes come in close contact. On the basis of comprehensive analyses, the model they proposed described a stepwise sequence that included cell recognition, initiation and formation of adhesion zippers between the two adjacent cells. In this model, two juxtaposed cells send out f-actin-filled filopodia that slide across each other after initial contact. The filopodia proceed to embed into the opposing cell membrane where the filopodia tips are stabilized by clusters of typical and atypical adherens junction proteins. Regions of membrane immediately adjacent on both sides of the nascent adherens junction are then clamped by desmosomes, which are the typical intermediate filament-based cell-cell junctions in keratinocytes consisting of DP as a main component. When DP is missing in keratinocytes, as was shown in epidermal-specific ablation of DP, membrane sealing is disrupted, as are cytoskeletal architecture and cell-cell adhesion (Vasioukhin et al., 2001). We show here that the first few steps of cell adhesion between endothelial cells in the process of making microvascular tubes appear similar to that described above for

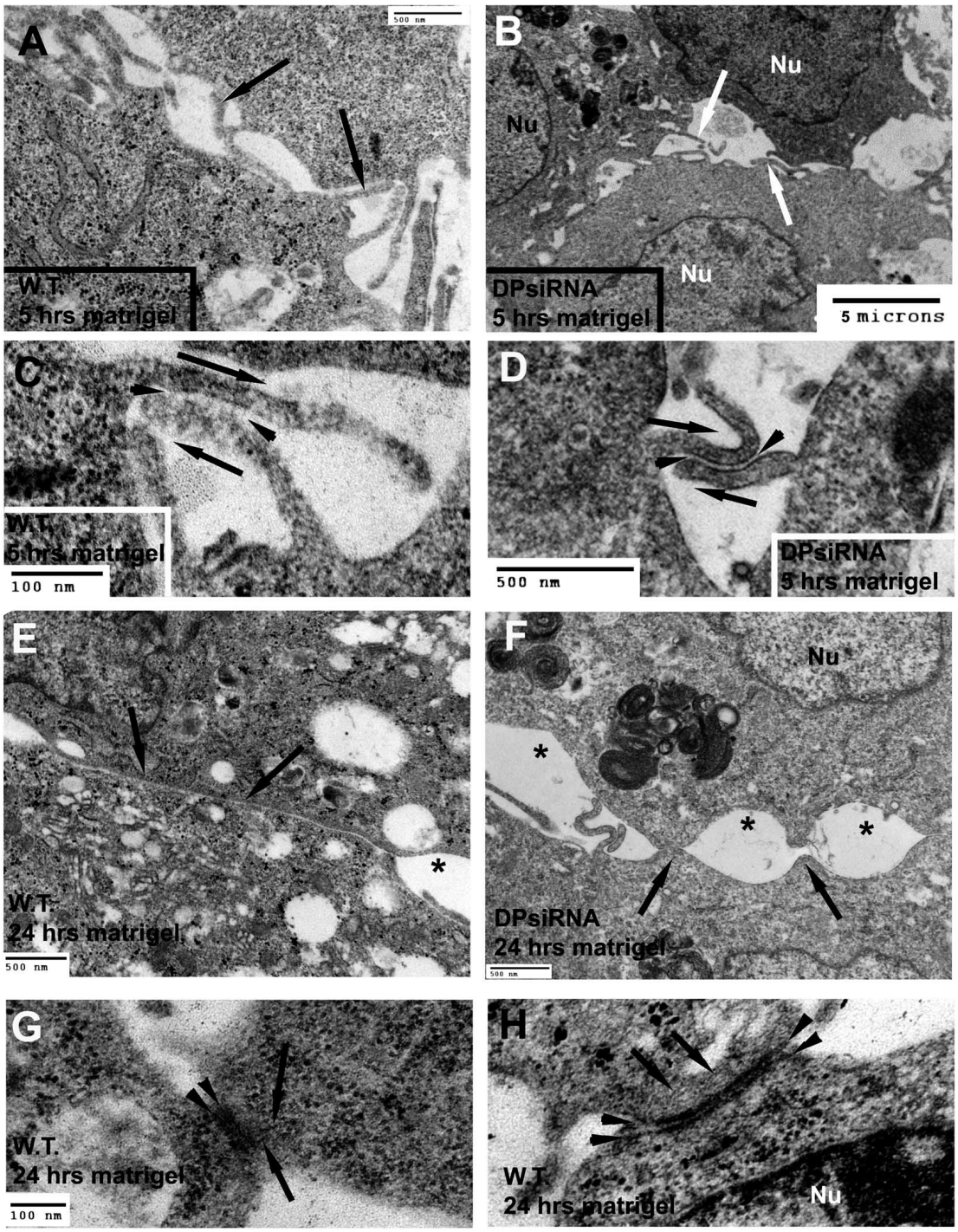

Fig. 9. Electron microscopy of HMEC-1 cells grown in culture with DP siRNA show distinct differences in cell-cell adhesion when compared with control cells. (A) Untreated, wild-type (w.t.) cells plated for 5 hours on matrigel showed distinct microvilli extending from each cell (arrows). (B) Arrows point to microvilli between cells treated with DPsiRNA. Note, cells come in close contact with each other. Nu, nucleus. (C) High-magnification view of two juxtaposed cells 5 hours after plating onto matrigel shows two microvilli (from A) sliding across each other. Arrows show direction of progress for each microvilli. Arrowheads point to distinct amorphous material adhering microvilli to each other. (D) DPsiRNA does not appear to compromise microvilli sliding or their adhesion to one another. An amorphous material similar to that seen in untreated cells (C) adhering two microvilli to each other was clearly visible (arrowheads). (E) Later stages of cell adhesion are evident 24 hours after plating onto matrigel. Areas of adhesion between untreated cells commonly spanned >3 μm (arrows), while areas of adhesion between DPsiRNA-treated cells rarely spanned beyond 500 nm (F). While some intercellular spaces were evident between untreated cells (asterisk in E), morphologically similar spaces were commonplace between DPsiRNA-treated cells (asterisks in F). (G-H) High-magnification views of complexus adherens junctions in untreated cells 24 hours after plating onto matrigel. Arrows point to filaments with diameters of ~10-12 nm (similar to vimentin) coming into close contact with electron dense plaques (arrowheads in G and H). Bar in G = 100 nm in H.

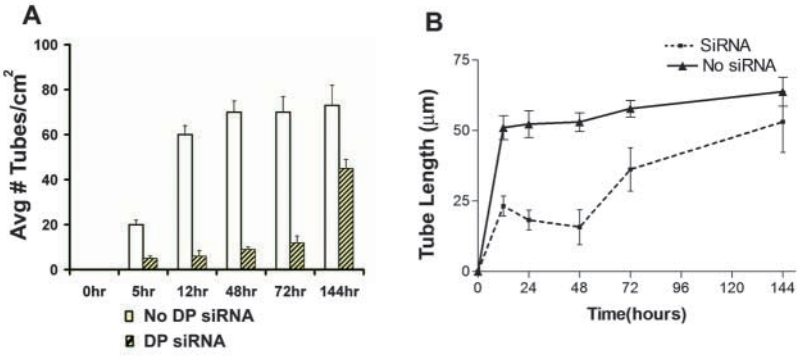

Fig. 10. Tube number and lengths were quantified. (A) Tubes were counted at increasing time points in a one cm^2 area from at least two wells per experiment. Each DP siRNA experiment was performed four times on both C166 cells and HMEC-1 cells. (B) Tube lengths were calculated over a 144 hour period.

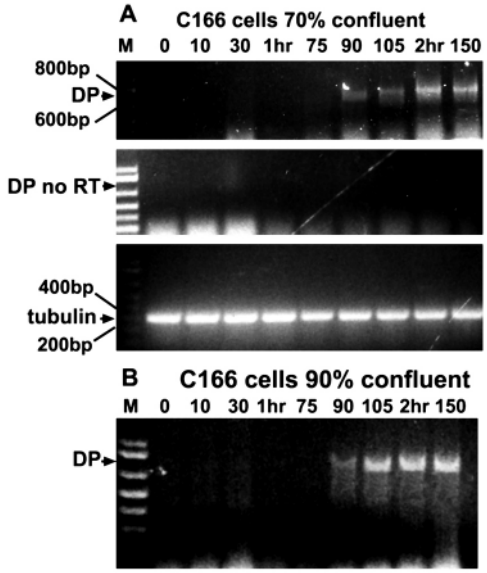

Fig. 11. DP gene expression in C166 cells was measured by RT-PCR. (A,B) The DMEM+serum medium normally used to grow C166 cells in monolayers was replaced with EGM-2 medium containing growth factors. Monolayers were placed back into the incubator for specified times. RT-PCR of these monolayers demonstrated that DP gene expression was first detected at 1.5 hours of incubation in both 70% (A) and 90% (B) confluent layers. Tubulin primers were used on the same samples as those used for DP to show the presence of mRNA in all samples. No RT controls also were performed on the same mRNA samples.

keratinocytes; that is, filopodia extension, recognition of adjacent cells and filopodia sliding. Using electron microscopy in an attempt to detail the latter steps of endothelial cell-cell recognition, we found in DP siRNA-treated cells that membrane sealing was compromised. Simple morphological observations of DPsiRNA-treated and untreated cells revealed many more intercellular spaces between treated cells as compared with untreated cells. However, the final steps of cell adhesion described by Vasioukhin et al. (Vasioukhin et al., 2000), i.e. clamping of apposing membranes by desmosomes, were not completely observed in our endothelial cell model systems, presumably because there are fewer complexus adherens junctions than desmosomes, making final observations extremely difficult to follow and accurately interpret.

In summary, we used novel siRNA technology to knock down DP protein expression in HMEC-1 endothelial cells. Normally, HMEC-1 cells and C166 cells form microvascular tubes when plated onto matrigel; however, with the addition of DP siRNA, tube formation in both cell types was significantly decreased. These results reveal that DP may be an excellent target for inhibiting angiogenesis in vivo especially in tumors, which need capillaries to survive.

We thank Dr Robert Lechleider, Dr Chris Taylor and Tammy Gallicano for their critical reading of the manuscript. We also thank Dr Hynda Kleinman for sending us matrigel. Work in this investigation was supported by the Histopathology and Tissue Shared Resource under the directorship of Dr Robert Russell who is supported by a Cancer Center Support Grant # CA51008-13. August Stuart is supported by a Training Grant in Tumor Biology # CA09686. This work was supported by grant # HL70204-01 from the NIH and a grant from the American Heart Association # O265429U, both awarded to G.I.G.

References

Ades, E. W., Candal, F. J., Swerlick, R. A., George, V. G., Summers, S., Bosse, D. C. and Lawley, T. J. (1992). HMEC-1, establishment of an immortalized human microvascular endothelial cell line. *J. Invest. Dermatol.* **99**, 683-690.

Bazzoni, G., Dejana, E. and Lampugnani, M. G. (1999). Endothelial adhesion molecules in the development of the vascular tree, the garden of forking paths. *Curr. Opin. Cell Biol.* **11**, 573-581.

Bosse, D., George, V., Candal, F. J., Lawley, T. and Ades, E. W. (1993). Antigen presentation by a continuous human microvascular endothelial cell line, HMEC-1, to human T cells. *Pathobiology* **61**, 236-238.

Calkins, C. C., Hoepner, B. L., Law, C. M., Novak, M. R., Setzer, S. V., Hatzfeld, M. and Kowalczyk, A. P. (2003). The armadillo family protein p0071 is a VE-cadherin- and desmoplakin-binding protein. *J. Biol. Chem.* **278**, 1774-1783.

Caplen, N. J., Parrish, S., Imani, F., Fire, A. and Morgan, R. A. (2001). Specific inhibition of gene expression by small double-stranded RNAs in invertebrate and vertebrate systems. *Proc. Natl. Acad. Sci. USA* **98**, 9742-9747.

Carmeliet, P. and Jain, R. K. (1999). Angiogenesis in cancer and other disease. *Nature* **407**, 249-257.

Cattelino, A., Liebner, S., Gallini, R., Zanetti, A., Balconi, G., Corsi, A., Bianco, P., Wolberg, H., Moore, R., Oreda, B. et al. (2003). The conditional inactivation of beta-catenin gene in endothelial cells causes a defective vascular pattern and increased vascular fragility. *J. Cell Biol.* **162**, 1111-1122.

Connolly, J. O., Simpson, N., Hewlett, L. and Hall, A. (2002). Rac regulates endothelial morphogenesis and capillary assembly. *Mol. Biol. Cell* **13**, 2474-2485.

Daub, H., Gavaert, K., Vandekerchkhove, J., Sobel., A. and Hall, A. (2001). Rac/Cdc42 and p65PAK regulate the microtubule-destabilizing protein stathmin through phosphorylation and serine 16. *J. Biol. Chem.* **276**, 1677-1680.

Davis, G. E., Black, S. M. and Bayless, K. J. (2000). Capillary morphogenesis

during human endothelial cell invasion of three-dimensional collagen matrices. *In Vitro Cell Dev. Biol.* **36**, 513-519.

Davis, G. E., Bayless, K. J. and Mavila, A. (2002). Molecular basis of endothelial cell morphogenesis in three-dimensional extracellular matrices. *Anat. Rec.* **268**, 252-275.

Dejana, E. (1996). Endothelial adherens junctions, implications in the control of vascular permeability and angiogenesis. *J. Clin. Invest.* **98**, 1949-1953.

Dejana, E., Corada, M. and Lampugnani, M. G. (1995). Endothelial cell-to-cell junctions. *FASEB J.* **9**, 910-918.

Dejana, E., Bazzoni, G. and Lampugnani, M. G. (1999). Vascular endothelial (VE)- cadherin, only an intercellular glue? *Exp. Cell. Res.* **252**, 13-19.

Elbashir, S. M., Harborth, J., Lendeckel, W., Yalcin, A., Weber, K. and Tuschl, T. (2001). Duplexes of 21-nucleotide RNAs mediate RNA interference in cultured mammalian cells. *Nature* **411**, 494-498.

Elbashir, S. M., Harborth, J., Weber, K. and Tuschl, T. (2002). Analysis of gene function in somatic mammalians cells using small interfering RNAs. *Methods* **26**, 199-213.

Gallicano, G. I., Kouklis, P. K., Bauer, C., Yin, M., Vasioukhin, V., Degenstein, L. and Fuchs, E. (1998). Desmoplakin is required early in development for assembly of desmosomes and cytoskeletal linkage. *J. Cell Biol.* **143**, 2009-2022.

Gallicano, G. I., Bauer, C. and Fuchs, E. (2001). Rescuing desmoplakin function in extra- embryonic ectoderm reveals the importance of this protein in embryonic heart, neuroepithelium, skin and vasculature. *Development* **128**, 929-941.

Haar, J. L. and Ackerman, G. A. (1971). A phase and electron microscopic study of vasculogenesis and erythropoises is in yolk sac of the mouse. *Anat. Rec.* **170**, 199-224.

Hatsell, S. and Cowin, P. (2001). Deconstructing desmoplakin. *Nature* **3**, E270-E272.

Hua, C. T., Gamble, J., Vadas, M. and Jackson, D. (1998). *J. Biol. Chem.* **273**, 28332-28340.

Ilan, N., Cheung, L., Pinter, E. and Madri, J. A. (2000). Platelet-endothelial cell adhesion molecule-1 (CD31), a scaffolding molecule for selected catenin family members whose binding is mediated by different tyrosine and serine/threonine phosphorylation. *J. Biol. Chem.* **275**, 21435-21443.

Kawasaki, H., Suyama, E., Iyo, M. and Taira, K. (2003). siRNAs generated by recombinant human Dicer induce specific and significant but target site-independent gene silencing in human cells. *Nucleic Acids Res.* **31**, 981-987.

Kouklis, P., Konstantoulaki, M. and Malik, A. (2003). VE-cadherin-induced Cdc42 signaling regulates formation of membrane protrusions in endothelial cells. *J. Biol. Chem.* **278**, 16230-16236.

Kowalczyk, A. P., Bornslaeger, E. A., Borgwardt, J. E., Palka, H. L., Dhaliwal, A. S., Corcoran, C. M., Denning, M. F. and Green, K. J. (1997). The amino-terminal domain of desmoplakin binds to plakoglobin and clusters desmosomal cadherin-plakoglobin complexes. *J. Cell Biol.* **139**, 773-784.

Kowalczyk, A. P., Navarro, P., Dejana, E., Bornslaeger, E. A., Green, K. J., Kopp, D. S. and Borgwardt, J. E. (1998). VE-cadherin and desmoplakin are assembled into dermal microvascular endothelial intercellular junctions, a pivotal role for plakoglobin in the recruitment of desmoplakin to intercellular junctions. *J. Cell Sci.* **111**, 3045-3057.

Kurzen, H., Moll, I., Moll, R., Schafer, S., Simics, E., Amagai, M., Wheelock, M. J. and Franke, W. W. (1998). Compositionally different desmosomes in the various compartments of the human hair follicle. *Differentiation* **63**, 295-304.

Leach, L., Babawale, M. O., Anderson, M. and Lammiman, M. (2002). Vasculogenesis, angiogenesis, and the molecular organization of endothelial junctions in the early human placenta. *J. Vasc. Res.* **39**, 246-249

Lu, L. S., Wang, S. J. and Auerbach, R. (1996). In vitro and in vivo differentiation into B cells, T cells, and myeloid cells of primitive yolk sac hematopoietic precursor cells expanded > 100-fold by coculture with a clonal yolk sac endothelial cell line. *Prac. Natl. Acad. Sci. USA* **93**, 14782-14787.

Maru, Y., Yamaguchi, S., Takahshi, T., Ueno, H. and Shibuya, M. (1998). Virally activated Ras cooperates with integrin to induce tubulogenesis in sinusoidal endothelial cell lines. *J. Cell. Physiol.* **176**, 223-234.

Matsumura, T., Wolff, K. and Petzelbauer, P. (1997). Endothelial cell tube formation depends on cadherin 5 and CD31 interactions with filamentous actin. *J. Immunol.* **158**, 3408-3416.

Myers, J. W., Jones, J. T., Meyer, T. and Ferrell, J. E. (2003). Recombinant Dicer efficiently converts large dsRNAs into siRNAs suitable for gene silencing. *Nat. Biotech.* **21**, 324-328.

Norgett, E. E., Hatsell, S. J., Carvajal-Huerta, L., Cabezas, J. C., Common, J., Purkis, P. E., Whittock, N., Leigh, I. M., Stevens, H. P. and Kelsell, D. P. (2000). Recessive mutation in desmoplakin disrupts desmoplakin-intermediate filament interactions and causes dilated cardiomyopathy, woolly hair and keratoderma. *Hum. Mol. Genet.* **9**, 2761-2766.

Pellegatta, F., Chierchia, S. L. and Zocchi, M. R. (1998). Functional association of platelet endothelial cell adhesion molecule-1 and phosphoinositide 3-kinase in human neutrophils. *J. Biol. Chem.* **273**, 27768-27771.

Pruckler, J. M., Lawley, T. and Ades, E. (1993). Use of human microvascular endothelial cell line as a model system to evaluate cholesterol uptake. *Pathobiology* **61**, 283-287.

Pumphrey, N. J., Taylor, V., Freeman, S., Douglas, M., Bradfield, P., Young, S., Lord, J., Wakelman, M. J. O., Bird, I., Salmon, M. et al. (1999). Differential association of cytoplasmic signalling molecules SHP-1, SHP-2, SHIP and phospholipase C-gamma1 with PECAM-1/CD31. *FEBS Lett.* **450**, 77-83.

Schmelz, M. and Franke, W. W. (1993). Complexus adhaerentes. A new group of desmoplakin-containing junctions in endothelial cells, the syndesmos connecting retothelial cells of lymph nodes. *Eur. J. Cell Biol.* **61**, 274-289.

Schmelz, M., Moll, R., Kuhn, C. and Franke, W. W. (1994). Complexus adhaerentes, a new group of desmoplakin-containing junctions in endothelial cells, II. Different types of lymphatic vessels. *Differentiation* **57**, 97-117.

Valiron, O., Chevrier, V., Usson, Y., Berruccio, B., Job, D. and Dejana, E. (1996). Desmoplakin expression and organization at human umbilical vein endothelial cell-to-cell junctions. *J. Cell Sci.* **109**, 2141-2149.

Vasioukhin, V., Bauer, C., Yin, M. and Fuchs, E. (2000). Directed actin polymerization is the driving force for epithelial cell-cell adhesion. *Cell* **100**, 209-219.

Vasioukhin, V., Bowers, E., Bauer, C., Degenstein, L. and Fuchs, E. (2001). Desmoplakin is essential in epidermal sheet formation. *Nat. Cell. Biol.* **3**, 1076-1085.

Venkiteswaran, K., Xiao, K., Summers, S., Calkins, C., Vincent, P. A., Pumiglia, K. and Kowalczyk, A. P. (2002). Regulation of endothelial barrier function and growth by VE-cadherin, plakoglobin, and bate- catenin. *Am. J. Physiol. Cell Physiol.* **283**, C811-C821.

Vittet, D., Buchou, T., Schweitzer, A., Dejana, E. and Huber, P. (1997). Targeted null-mutation in the vascular endothelial-cadherin gene impairs the organization of vascular-like structures in embryoid bodies. *Proc. Natl. Acad. Sci. USA* **94**, 6273-6278.

Wang, S. J., Greer, P. and Auerbach, R. (1996). Isolation and propagation of yolk-sac-derived endothelial cells from a hypervascular transgenic mouse expressing a gain-of-function FPS/FES proto-oncogene. *In Vitro Cell. Dev. Biol.* **32**, 292-299.

Xu, Y. L., Swerlick, R. A., Sepp, N., Bosse, D., Ades, E. W. and Lawley, T. J. (1994). Characterization of expression and modulation of cell adhesion molecules on an immortalized human dermal miceovascular endothelial cell line (HMEC-1). *J. Invest. Dermatol.* **102**, 833-837.

Yang, S., Graham, J., Kahn, J. W., Schwartz, E. A. and Gerritsen, M. E. (1999). Functional roles for PECAM-1 (CD31) and VE-Cadherin (CD144) in tube assembly and lumen formation in three-dimensional collagen gels. *Am. J. Pathol.* **155**, 887-895.